

Digitally Controlled Phase Shifter using an SOI Slot Waveguide with Liquid Crystal Infiltration

Yufei Xing, Thomas Ako, *Student Member, IEEE*, John P. George, *Student Member, IEEE*, Dietmar Korn, Hui Yu, Peter Verheyen, Marianna Pantouvaki, Guy Lepage, Philippe Absil, Alfonso Ruocco, Christian Koos, Juerg Leuthold, *Fellow, IEEE*, Kristiaan Neyts, Jeroen Beeckman, *Member, IEEE*, Wim Bogaerts, *Senior Member, IEEE*

Abstract—We demonstrate a phase shifter using a silicon slot waveguide infiltrated with liquid crystal. For a 1 mm long device we achieve 73π phase shift with a 5 V voltage, with a voltage-length product of 0.0224 V·mm around 1 V. We drive the phase shifter with a digital 1 V, duobinary pulse-width-modulated signal, or a 1 V frequency-modulated signal. This enables direct digital CMOS control of an analog optical phase shifter.

Index Terms—Silicon Photonics. Slot Waveguide. Liquid Crystal. Phase modulator

I. INTRODUCTION

Optical phase shifters in silicon are usually based on thermal or plasma-dispersion effects [1], which are generally quite weak (having a high $V_\pi \cdot L_\pi$ product), requiring long phase shifters or high driving voltages. Hybrid devices combining silicon with electro-optic materials can have a much higher efficiency, and various examples have been demonstrated using slot waveguides filled with electro-optic polymers [2], [3]. For modulation, the first criterium is efficiency and operation speed, but for tuning and switching power consumption is a greater concern. We present an optical phase shifter based on a silicon slot waveguide infiltrated with liquid crystal. Compared to other organic electro-optic materials, liquid crystals exhibit a very strong but slow electro-optic effect. Tuning of silicon waveguides based on liquid crystals has been demonstrated before [4], [5], [6]. A liquid crystal in a slot waveguide increases the confinement of light in the LC and at the same time the electric field strength between the LC electrodes, dramatically reducing the switching voltage [7].

YX, JPG, HY, AR, WB are with the Photonics Research Group, Ghent University - imec, Department of Information Technology, Ghent, Belgium. YX, TA, JPG, KN, JB are with the Liquid Crystal and Photonics Group, Ghent University, Department of Electronics and Information Systems, Ghent, Belgium. DK, CK and JL are with Karlsruhe Institute of Technology (KIT), Institutes IPQ and IMT, Engesserstr. 5, 76131 Karlsruhe, Germany. PV, MP, GL and PA are with IMEC vzw, Leuven, Belgium. YX, TA, JPG, HY, JB and WB are also with the Center of Nano- and Biophotonics (NB-photonics), Ghent, Belgium.

Some authors have changed affiliations since: DK is now with Imagine Optic, Paris, France. HY is now with Zhejiang University, Department of Information Science and Electronic Engineering, Hangzhou 310027, China. JL is now with the Electromagnetic Fields Laboratory, Swiss Federal Institute of Technology (ETH), Zurich, Switzerland. WB is now part-time with Luceda Photonics, Dendermonde, Belgium.

Part of this research was funded by the European Union in the context of the 7th Framework Project FP7-SOFI

Manuscript received September 25, 2014; revised January 7, 2015. First published March 15, 2015.

The accuracy of the electrical control of the phase shifter is very important, and the precision and linearity of a digital-to-analog converter can easily become a limiting factor. Instead of a DAC circuit, we use the limited response time of the liquid crystal to convert a digital drive signal into an analog phase modulation. Using a fast 1 V pulse-width-modulated (PWM) signal, we demonstrate a 30π phase shift in a 1 mm device, as we already summarily reported in [8]. Alternatively, we demonstrate a similar phase shift using frequency modulation of a 1 V digital AC signal.

II. CONCEPT AND DESIGN

The concept of our device is shown in Fig. 1. We embedded the phase shifter in a Mach-Zehnder interferometer (MZI), so we can measure a phase shift by observing the amplitude modulation. To balance the losses, both arms have a phase shifter, but we keep one arm shorted and grounded. The slot waveguides provide both high electrical and high optical confinement. The narrow slot width ($\sim 150\text{nm}$) results in a high electric field to reorient the liquid crystal molecules. We simulated the device using a finite element based Q-tensor model [9]. Fig. 2 shows both the electric potential in the liquid crystal and the orientation of the liquid crystal director. It shows that, without a voltage, the liquid crystal molecules align with the silicon slot waveguide. With a voltage of 2 V we see a reorientation in the slot. We used the properties of E7 liquid crystal for this simulation, the same material as we use further in the experiment [10].

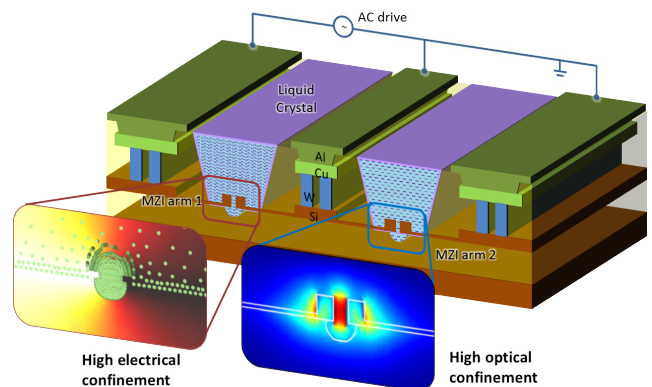


Fig. 1. Conceptual cross section drawing: The two arms of the Mach-Zehnder Interferometer have a slot waveguide infiltrated with liquid crystal.

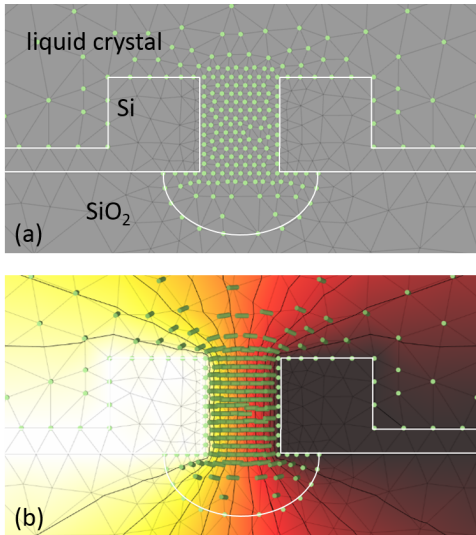


Fig. 2. Simulation of the E7 liquid crystal in the slot waveguides. The color background indicates the local electrical potential (a) Orientation of the LC molecules without bias, and (b) when a voltage is applied.

The slot waveguide also gives a very strong optical confinement for the TE mode of the waveguide. We simulated the optical mode using the full anisotropy of the liquid crystal in the slot waveguide [11], and Fig. 3 shows how most of the light is confined in the slot. The large overlap of the light with the liquid crystal will result in a very strong modulation of the effective index. Fig. 4 shows the simulated change in effective index of the TE mode when increasing the voltage over the slot. We obtain a change in n_{eff} of over 0.05. However, the dependence of Δn_{eff} on voltage depends strongly on the anchoring energy of the liquid crystal to the silicon sidewalls.

III. FABRICATION

The Mach-Zehnder devices were designed at Karlsruhe Institute of Technology and fabricated in IMEC. The slots are patterned using a 220 nm silicon etch, while the waveguides are etched only 150 nm on the side, allowing electrical contacting. The silicon is n-doped in the core, with a higher doping and silicidation further away from core [12]. A top cladding of $1\mu m$ of silicon dioxide is deposited. The electrode fabrication uses a damascene process with tungsten vias and copper wires, finished with aluminium-copper pads. After passivation, the cladding is etched back using a dry etch process and a buffered-HF wet etch, opening the slot waveguide.

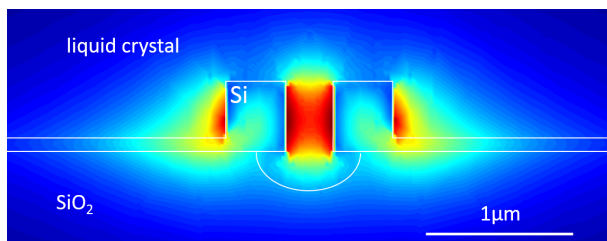


Fig. 3. Intensity profile of the TE mode in the slot waveguide without voltage.

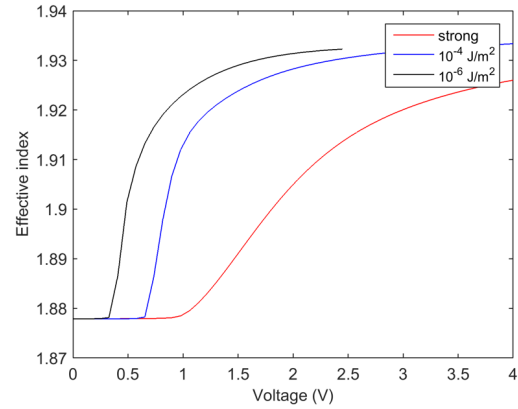


Fig. 4. Simulation of the effective index of the TE mode when applying a voltage over the liquid crystal in the slot waveguide, for different anchoring strengths of the silicon surface.

The resulting cross section is shown in Fig. 5, with a slight undercut in the buried oxide

After opening the top cladding, the liquid crystal is applied directly on the chip. It is difficult to verify whether the slot is completely filled, but from the experiment we can assume that the infiltration is quite efficient. The slight undercut is most likely also beneficial for the infiltration.

IV. DEVICE CHARACTERIZATION

We measured the optical transmission of the device by coupling light in using a fiber grating coupler and coupling the light out through another grating coupler. At the same time, we electrically probe the sides of the slot waveguides. After probing, we deposit a drop of liquid crystal. This is shown in Fig. 6 and Fig. 7. When applying a voltage over one arm, the phase shift will result in an intensity change at the MZI output. We operate the phase shifter in alternating current (AC), to avoid the buildup of an ionic charge layer. The AC frequency is between 30 kHz and 1 MHz, beyond which the response of the E7 liquid crystal is too small [13], [10].

A. Optical Transmission

The grating couplers have a peak efficiency of -5.5 dB each at 1510 nm, but maintaining optimal alignment after liquid crystal deposition was difficult in our experimental setup. The on-chip loss of the Mach-Zehnder interferometers is -11 ± 1 dB, which includes the splitter and combiner. From this, we

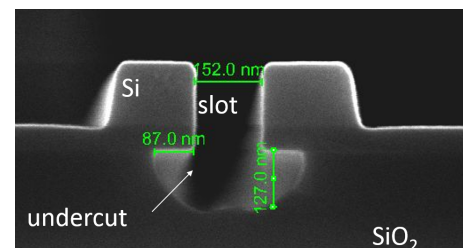


Fig. 5. SEM cross section of the slot waveguide after back-end opening.

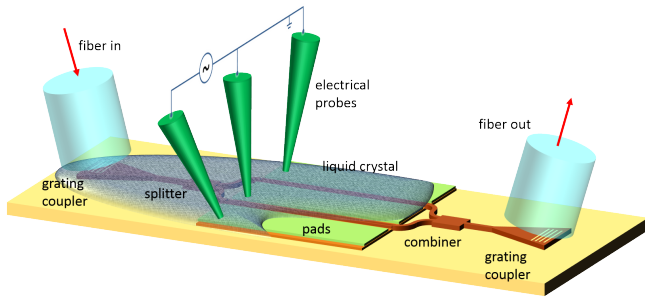


Fig. 6. Schematic of the measurement of the liquid crystal phase shifter. To characterize the phase modulator, the electrodes over one arm are shorted and grounded.

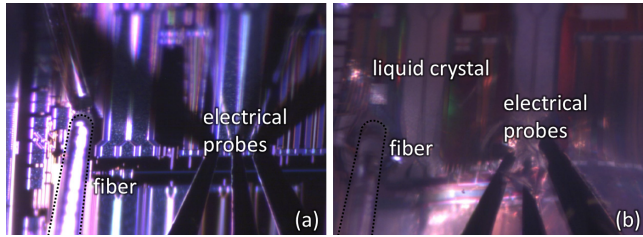


Fig. 7. Microscope image of the chip with fiber and electrical probes (a) before applying the liquid crystal, and (b) after applying the liquid crystal.

estimate the loss of the 1 mm phase shifter to -10 ± 1 dB, including the strip-to-slot waveguide transitions.

B. Phase response

We characterized the static response by sweeping the AC amplitude from 0-5 V over 0.5 seconds, while we observed the intensity modulation, recording the peaks and zeros corresponding to a 0 and π phase difference. The resulting phase shift, in multiples of π , is plot in Fig. 8. For 5 V we achieve a modulation of 73π , where the effect saturates. This indicates a complete reorientation of the liquid crystal molecules. Fig. 9 shows the modulation efficiency, expressed in π phase shift per volt (for the 1 mm phase shifter), as a function of the bias voltage. We have the highest modulation efficiency around 1 V, with a differential phase shift of $d\phi/dU = 44.53\pi/V$, corresponding to a voltage-length product of 0.0224 V·mm.

C. Switching time and power consumption

We measured the switching time of the device from an off-state to a nearby on-state and back. The switch-on and switch-off time is between 1.4 ms and 2.5 ms, but we see no clear dependence on the bias voltage between 0.2 V and 2.7 V. De transients between 2.4 V and 2.5 V are shown in Fig. 10. When we apply a 4 V pre-emphasis, we can reduce the switching time to 100 μs , but this complicates the control. The power consumption of charging the slot capacitor is extremely low and difficult to measure directly. We could deduce an upper limit of 2 nW.

V. DIGITAL CONTROL

Instead of using an analog control of the phase shifter, we explored the use of a digital signal. This is possible because

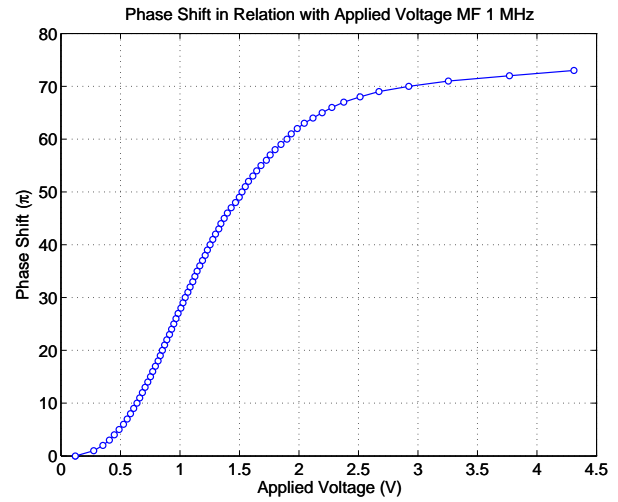


Fig. 8. Phase shift as a function of control voltage. A phase shift of 73π is achieved at drive voltage of 5 V.

of the high modulation efficiency and the good response of the phase shifter at low voltages. The relatively slow response enables digital averaging, rather than a dedicated digital-to-analog circuit. We present two control strategies: pulse-width modulation (PWM) and frequency modulation (FM).

A. Pulse-width modulation (PWM)

With pulse-width modulation, we use the duty-cycle of a digital train to control the average voltage. The LC will respond only to the RMS of the voltage. The precision of the control is determined by the word length, with the requirement that the word should be much shorter than the switching time. We used a word rate of 25.6 kHz. One complication is that the liquid crystal requires an AC signal with a net zero voltage. Therefore, we use duobinary encoding where pulses are alternatingly positive or negative, as shown in Fig. 11. We sweep the duty cycle of the PWM and record the output of the MZI, measuring the oscillations between constructive and destructive interference. The observed phase shift as function

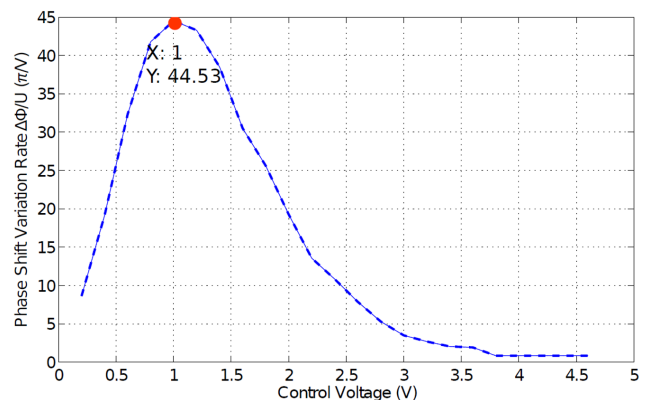


Fig. 9. Small signal modulation efficiency of a 1 mm long phase shifter as function of bias voltage. A maximum efficiency of $44.53\pi/V$ is observed, corresponding to a modulation efficiency of $V_{\pi} \cdot L_{\pi} = 0.0224V \cdot mm$

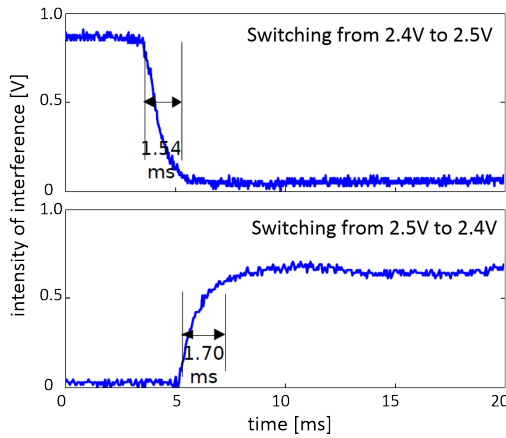


Fig. 10. Transient switch-on and switch-off transmission (Applying a π phase shift between a drive voltage of 2.4 V and 2.5 V)

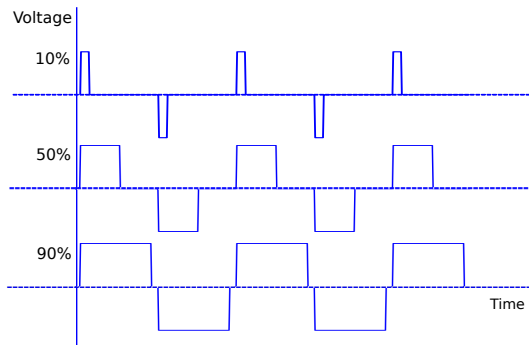


Fig. 11. Duobinary PWM drive signal.

of duty cycle for 1 V is shown in Fig. 12. For the 1 mm phase shifter we observe a maximum of 32π phase shift.

B. Frequency Modulation (FM)

An alternative control scheme relies on the decrease in response of the liquid crystal at higher frequencies. This effect depends on the bias voltage [13]. With a constant 1 V AC drive voltage but changing the AC frequency, we can control the phase shift. In Fig. 13 we sweep between 200 kHz and 1 MHz and we observe a -30π difference in phase shift, with a quite linear response with frequency.

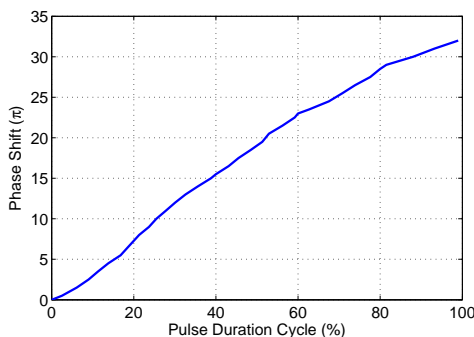


Fig. 12. Phase shift with increasing duty cycle of the PWM drive signal at 1.0V. We observe a phase shift of 32π .

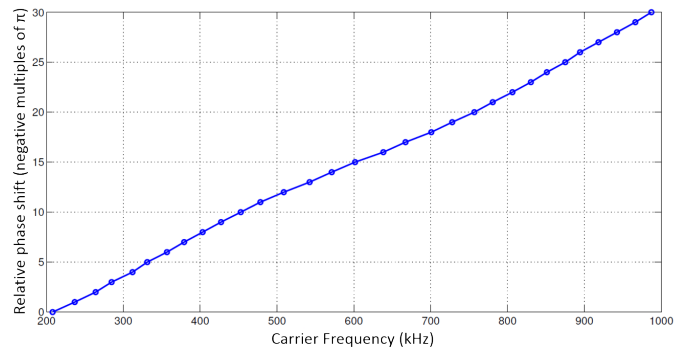


Fig. 13. Induced phase shift as a function of the AC frequency with constant amplitude of 1 V, relative to the shift at 200 kHz. Up to -30π phase shift can be obtained between 200 kHz and 1 MHz.

VI. CONCLUSION

We have demonstrated an efficient phase shifter using a silicon slot waveguide with liquid crystal filling. The modulation efficiency is $0.0224 \text{ V}\cdot\text{mm}$, and we controlled the device directly with digital signals using PWM and frequency modulation. With a 1 V drive voltage we achieve 30π phase shift over 1 mm, which means a 2π phase shifter can be realized in $70 \mu\text{m}$.

REFERENCES

- [1] G. T. Reed, G. Mashanovich, F. Y. Gardes, and D. J. Thomson, "Silicon optical modulators," *Nature Photonics*, vol. 4, no. 8, pp. 518–526, Aug. 2010.
- [2] J. Leuthold, C. Koos, W. Freude, L. Alloati *et al.*, "Silicon-organic hybrid electro-optical devices," *J. Sel. Top. Quantum Electron.*, vol. 19, no. 6, pp. 114–126, Nov 2013.
- [3] R. Ding, T. Baehr-Jones, Y. Liu, R. Bojko *et al.*, "Demonstration of a low V pi L modulator with GHz bandwidth based on electro-optic polymer-clad silicon slot waveguides," *Opt. Express*, vol. 18, no. 15, pp. 15 618–15 623, Jul. 19 2010.
- [4] J. Ptasinski, S. Kim, L. Pang, I. Khoo *et al.*, "Optical tuning of silicon photonic structures with nematic liquid crystal claddings," *Opt. Lett.*, vol. 38, pp. 2008–2010, 2013.
- [5] C. Wang, Y. Li, J. Yu, C. Wang *et al.*, "Electrically tunable high Q-factor micro-ring resonator based on blue phase liquid crystal cladding," *Opt. Express*, vol. 22, pp. 17 776–17 781, 2014.
- [6] W. De Cort, J. Beeckman, T. Claes, K. Neyts *et al.*, "Wide tuning of silicon-on-insulator ring resonators with a liquid crystal cladding," *Opt. Lett.*, vol. 36, no. 19, pp. 3876–3878, Oct 2011.
- [7] J. Pfeifle, L. Alloati, W. Freude, J. Leuthold *et al.*, "Silicon-organic hybrid phase shifter based on a slot waveguide with a liquid-crystal cladding," *Opt. Express*, vol. 20, no. 14, pp. 15 359–15 376, 2012.
- [8] Y. Xing, T. Ako, J. George, D. Korn *et al.*, "Direct digital control of an efficient silicon+liquid crystal phase shifter," in *Group IV Photonics 2014*, 2014, pp. 43–44.
- [9] R. James, E. Willman, F. Anbal Fernandez, and S. Day, "Finite-element modeling of liquid-crystal hydrodynamics with a variable degree of order," *IEEE T. Electron Dev.*, vol. 53, pp. 1575–1582, 2006.
- [10] M. Okutan, O. Köysal, S. San, and Y. Köysal, "Electrical parameters of different concentrations of methyl red in fullerene doped liquid crystal," *ISRN Nanomaterials*, 2012.
- [11] J. Beeckman, R. James, F. Fernandez, W. De Cort *et al.*, "Calculation of fully anisotropic liquid crystal waveguide modes," *J. Lightwave Technol.*, vol. 27, no. 17, pp. 3812–3819, Sept. 2009.
- [12] P. Verheyen, M. Pantouvaki, J. Van Campenhout, P. P. Absil *et al.*, "Highly uniform 25 Gb/s Si photonics platform for high-density, low-power wdm optical interconnects," in *Integrated Photonics Research, Silicon and Nanophotonics*, 2014, pp. IW3A–4.
- [13] M. Van Bostel, M. Wübbenhorst, J. Van Turnhout, C. Bastiaansen *et al.*, "A dielectric study on the relaxation and switching behaviour of liquid crystals confined within a colloidal network," *Liquid crystals*, vol. 30, no. 2, pp. 235–249, 2003.